Microtubules and Actin Filaments Are Not Critically Involved in the Biogenesis of Epithelial Cell Surface Polarity

Pedro J. I. Salas,* David E. Misek,‡ Dora E. Vega-Salas,* Doris Gundersen,* Marcelino Cereijido,§ and Enrique Rodriguez-Boulan*

*Department of Cell Biology and Anatomy, Cornell University Medical College, New York, New York 10021; ‡Department of Pathology, Downstate Medical Center, State University of New York, Brooklyn, New York 11203; §Centro de Investigacion y de Estudios Avanzados del Instituto Politecnico Nacional, Apartado Postal 14-740, Mexico, 14 D. F.

Abstract. We have studied the role of microtubules and actin filaments in the biogenesis of epithelial cell surface polarity, using influenza hemagglutinin and vesicular stomatitis G protein as model apical and basolateral proteins in infected Madin-Darby canine kidney cells. Addition of colchicine or nocodazole to confluent monolayers at concentrations sufficient to completely disassemble microtubules did not affect the asymmetric budding of influenza or vesicular stomatitis virus and only slightly reduced the typical asymmetric surface distribution of their envelope proteins, despite extensive cytoplasmic redistribution of the Golgi apparatus. Alteration of microtubular function by taxol or dissociation of actin filaments by cytochalasin D also failed to have a significant effect. Furthermore, neither colchicine nor cytochalasin D pretreatment blocked the ability of subconfluent Madin-Darby canine kidney cells to sustain polarized budding of influenza virus a few hours after attachment to the substrate. Our results indicate that domain-specific microtubule or actin filament "tracks" are not responsible for the vectorial delivery of apically or basolaterally directed transport vesicles. In conjunction with currently available evidence, they are compatible with a model in which receptors in the cytoplasmic aspect of apical or basolateral regions provide vectoriality to the transport of vesicles carrying plasma membrane proteins to their final surface localization.

EPITHELIAL cells display a striking polarization of their plasma membranes into two different domains, apical and basolateral, with different ultrastructure, function, and biochemical composition (63, 76). The boundary between the two regions is given by the tight junctions or zonulae occludentes (17, 23). The nature of the mechanisms responsible for this surface polarization is still unknown.

Cell lines that reproduce in culture polarity properties of parental epithelia, such as Madin-Darby canine kidney (MDCK),[1] provide excellent systems to study the origin of epithelial cell polarity (9, 29, 37, 47, 60). Furthermore, when these cell lines are infected with enveloped RNA viruses, a strikingly asymmetric viral assembly is observed. Influenza virus and several paramyxoviruses bud from the apical domain of the plasma membrane, while vesicular stomatitis virus (VSV) assembles from basolateral regions (68). Polarized viral budding appears to be mainly determined by the asymmetric localization of viral envelope glycoproteins in the plasmalemma, e.g., influenza hemagglutinin (HA) is concentrated in the apical surface and VSV G protein in the basolateral surface (65). Recent work indicates that apical and basolateral viral glycoproteins follow the same pathway to the Golgi apparatus where they co-distribute (19, 61, 72). They are then sorted intracellularly, presumably at a late Golgi stage, incorporated into specific transport vesicles, and vectorially exocytosed to the respective target surface (43, 44, 46, 55, 62, 67, 72).

The involvement of microtubules and microfilaments in secretion has been demonstrated by drug inhibition studies. Dissociation of actin microfilaments with cytochalasin D (4) or of microtubules with colchicine (33, 34, 41, 51, 53, 75) inhibit regulated secretion in various epithelial glandular cells, as well as nonregulated secretion by fibroblasts (13, 16) or liver cells (58). This correlates with a dramatic alteration in the structure of the Golgi apparatus caused by antimicrotubular agents, like colchicine, nocodazole, and taxol (8, 11, 49, 52, 69, 82).

Because plasma membrane glycoproteins, including viral envelope proteins, use segments of the secretory pathway during their biogenesis (38, 63, 71) and because microtubules play a well demonstrated role in the cytoplasmic transport of organelles (1, 30, 73, 74), the intracellular migration of plasma

1. *Abbreviations used in this paper:* BHK, baby hamster kidney; DME, Dulbecco's modified Eagle's medium; FCS, fetal calf serum; HA, hemagglutinin; MDCK, Madin-Darby canine kidney; NBD, nitrobenzooxidazole; PHEMGT buffer, 60 mM Pipes, 25 mM Hepes, 8 mM EGTA, 2 mM $MgCl_2$, 0.5 mM GTP, 10 μM taxol, pH 6.9; RIA, radioimmunoassay; TMER, transmonolayer electrical resistance; VSV, vesicular stomatitis virus.

membrane proteins and, in particular, their vectorial delivery to specific epithelial cell surfaces, might also be controlled by the cytoskeleton. Specifically, it may be hypothesized that distinct sets of cytoskeletal elements provide "transport tracks" for apically or basolaterally directed post Golgi vesicles. Available evidence in this regard is contradictory. Quaroni et al. (56) have reported an inhibitory effect of colchicine on the intracellular transport of apical glycoproteins in intestinal epithelial cells. On the other hand, Griffin and Compans (25) and Genty and Bussereau (22) found no effect of cytochalasin B or colchicine on the maturation of influenza and VSV from cultured cells, and Rogalski et al. (70) reported no inhibition by nocodazole or taxol of the intracellular transport of VSV G protein in fibroblasts.

Pieces of circumstantial evidence also suggest a possible role for the cytoskeleton in maintaining plasma membrane polarity in epithelial cells. Namely, tight junctions are associated with cytoskeletal elements, mostly actin and alpha-actinin (6, 12, 21, 39, 45), and the electrical resistance of tight junctions drops in the presence of cytochalasin B (10, 45, 50).

In this study, we have analyzed the effect of antimicrotubular and antimicrofilament agents on the polarized budding of viruses and on the intracellular transport and asymmetric surface distribution of apical and basolateral viral glycoproteins in MDCK cells infected with influenza virus or VSV. Our results do not support a critical involvement of either type of cytoskeletal element in the establishment or maintenance of epithelial cell surface polarity.

Materials and Methods

Cell Lines

MDCK cells were grown in high glucose Dulbecco's modified Eagle's medium (DME) (GIBCO, Grand Island, NY) supplemented with 10% fetal calf serum (FCS) (GIBCO) or 10% horse serum and antibiotics. Two strains of MDCK cells were used: low resistance or strain II, and high resistance or strain I (59). Strain I MDCK cells were obtained from Dr. N. Simmons, Glasgow, Scotland and cloned by dilution: clone 6, which developed transmonolayer electrical resistances (TMER) above 1,000 ohms·cm^2 after 3 d of confluence, was used for the experiments in this paper. For spinner culture experiments, monolayers of MDCK or baby hamster kidney (BHK) cells were dissociated with 0.1% trypsin, 0.5 mM EDTA in Moscona's saline buffer, centrifuged in DME that contained 10% FCS, and resuspended in DME that contained 0.2% bovine serum albumin (BSA). The cells (4×10^5 cells/ml) were immediately transferred to a siliconized spinner flask and incubated overnight at 50–60 rpm in a 5% CO_2/air incubator at 37°C. Under these suspension conditions cells did not divide or aggregate and were mostly viable (90%, as determined by trypan blue exclusion) after 6 h or by the following day. VERO cells were grown in DME, 5% FCS.

Viruses and Viral Infections

Influenza (WSN strain), VSVs, and their temperature mutants Ts61 and TsO45 were grown as described elsewhere (64, 67). TsO45 infection of clone 6 MDCK cells was done with virus adapted and titered in these cells. For experiments, MDCK monolayers confluent for 2–3 d were infected with wild type viruses at 37°C, or with the temperature-sensitive mutants at 40°C (nonpermissive temperature), in a 5% CO_2/air incubator in DME that contained 0.2% BSA. Inoculations with VSV or its Ts mutant were done in the presence of 50–100 μg/ml DEAE dextran; ~75% of the cells were infected under the conditions used in this paper. In temperature shift experiments, transfer from the nonpermissive to the permissive temperature was done by replacing the medium at 40°C by medium prewarmed at 32°C.

Drugs and Doses

The following drugs and doses were used: colchicine (Sigma Chemical Co., St. Louis, MO) 20 μM; nocodazole (Aldrich Chemical Co., Milwaukee, WI) 33 μM; taxol (National Institutes of Health, National Cancer Institute, Bethesda, MD, lot no. FB1046) 14 μM; cytochalasin D (Sigma Chemical Co.) 39 μM. The doses of anticytoskeletal agents used in this work, although high, are similar to those previously used in other systems. Rogalski et al. (69, 70) used 30 μM nocodazole and 10 μM taxol on normal rat kidney cells. Madara (40) used 10 μM cytochalasin D on intestinal epithelium; Andrews (2) used doses as high as 20 and 50 μM cytochalasin D on kidney glomerular podocytes; Knapp et al. (36) used 1 μM cytochalasin D on endothelial cells. The dose of colchicine (20 μM) has been found to be maximal in MDCK cells (45); however, Ojakian (50) reported effects on the transepithelial electrical resistance with 0.1 μM colchicine.

Preparation of Detergent-extracted Cytoskeletons

To determine the effect of antimicrotubular agents, confluent MDCK monolayers were treated for 90 s with 0.5% Triton X-100 in PHEMGT buffer (60 mM Pipes, 25 mM Hepes, 8 mM EGTA, 2 mM $MgCl_2$, 0.5 mM GTP, 10 μM taxol, pH 6.9) (57), fixed with methanol for 5 min at −20°C, and processed for either indirect immunofluorescence or indirect radioimmunoassay (RIA).

Antibodies

A monoclonal antibody against beta-tubulin produced by S. Blose, Cold Spring Harbor (5), was used to characterize the effect of antimicrotubular drugs by indirect immunofluorescence and indirect RIA. Rabbit polyclonal HA and G antibodies were prepared as described before (46). Hybridomas that produce monoclonal anti-HA and anti-G antibodies were kindly donated by Dr. Walter Gerhardt, Winstar Institute, PA, and Dr. Robert R. Wagner, University of Virginia, Charlottesville, VA, respectively. Fab fragments of rabbit anti-HA and rabbit anti-G IgGs were prepared as previously described (46) and iodinated by the chloramine-T procedure; free iodine was removed on a PD-10 column (Pharmacia Fine Chemicals, Piscataway, NJ). Iodinated Fab fragments were affinity purified on infected monolayers of MDCK cells (influenza) or Vero cells (VSV) fixed with formaldehyde.

Semithin Frozen Sections

Glass coverslips (25 cm^2) were covered with a thin layer of collagen cross-linked by exposure to ammonium hydroxide vapors, sterilized in 1% glutaraldehyde, extensively washed in phosphate-buffered saline (PBS), and incubated in DME to block aldehyde groups. Strain II or strain I (clone 6) MDCK cells were plated at confluence, incubated at 37°C for 2 or 3 d, and infected, respectively, with influenza virus (moi = 10) for 6.5 h at 37°C or with TsO45 (moi = 40) for 4 h at 40°C followed by 3 h at 32°C. Anticytoskeletal drugs were added at 2.5 h of infection and kept throughout the whole experiment. The monolayers were then fixed in 2% formaldehyde (freshly prepared from paraformaldehyde), scraped, embedded in 5% gelatin at 37°C, and infiltrated at 4°C with 1.5 M sucrose overnight. 0.5-μm sections were cut at −60°C with glass knives in a Sorvall MT-5000 microtome equipped with a cryostat attachment (Sorvall FS1000), picked up in a frozen droplet of 1.5 M sucrose with a wire loop, and placed on polylysine-coated coverslips. After postfixation in 2% formaldehyde, they were stained for immunofluorescence.

Immunofluorescence

Immunofluorescence staining of monolayers grown on glass coverslips or of frozen sections prepared as described above was done by an indirect technique (for complete procedure see reference 64). Cell monolayers were fixed with 2% formaldehyde (freshly prepared from paraformaldehyde) in PBS that contained 0.1 mM $CaCl_2$ and 1 mM $MgCl_2$ (PBS-CM) at room temperature and, when necessary, permeabilized with 0.2% Triton X-100 (Bio-Rad Laboratories, Richmond, CA) in PBS. Aldehyde groups were quenched with 50 mM NH_4Cl in PBS (used for both monolayers or frozen sections). First and second antibodies were added in PBS that contained 0.1% albumin. Second antibodies were affinity purified goat anti-mouse or goat anti-rabbit IgG coupled to rhodamine (Cappel Laboratories, Cochranville, PA). Actin microfilaments were stained in one step with nitrobenzooxidazole (NBD) phallacidin (Molecular Probes, Inc., Eugene, OR). The coverslips were mounted on glass slides in 20% Gelvatol (Monsanto Co., St. Louis, MO) in PBS that contained 15% glycerol, examined with a Leitz Ortholux epifluorescence microscope, and photographed on Kodak Tri-X 400 ASA film.

Recording of TMER

TMER, a measure of the integrity of the tight junctions, was determined in Ussing type chambers adapted to hold nitrocellulose filter chambers (described in reference 46) from the voltage deflection generated by the passage of 20 μAmp via $AgCl_2$ coated silver electrodes.

RIA

The procedure for indirect RIA of antigens in monolayers grown on plastic petri dishes was done as described elsewhere (67). Measurement by RIA of microtubular tubulin content was done in confluent monolayers extracted for 90 s with 0.5% Triton X-100 in PHEMGT buffer and fixed with pure methanol for 5 min at −20°C. The monolayers were incubated with a monoclonal tubulin antibody (30 min) in the first step and with affinity purified ^{125}I-goat anti-mouse IgG in the second step. To determine by direct RIA the amounts of HA and G in the apical and basolateral membranes, MDCK cells were grown on nitrocellulose filter chambers as described elsewhere (46). Monolayers of strain I or II MDCK cells confluent for 2 or 3 d (with daily medium changes) were inoculated, respectively, with influenza (moi = 10) for 6.5 h at 37°C or with TsO45 (moi = 40) for 4 h at 40°C followed by 3 h at 32°C. The monolayers were fixed as with formaldehyde as described above, and the aldehyde groups were quenched with 50% mM lysine in PBS-CM. We observed in direct immunofluorescence experiments that Fab fragments of anti-G antibodies had better accessibility than whole IgG molecules through the filters to the lateral surface and gave ring images that spanned the entire thickness of the monolayer, as seen by changing the focal plane with a 63× lens. Therefore, we used iodinated Fab fragments for the RIAs on filter chambers. Ideal accessibility to the basolateral surface was observed under stirring: for this purpose, groups of five chambers were glued from the top to the cover of a 60-mm petri dish (previously perforated to allow access to the apical compartment) with Millex cement formulation 1 (Millipore Corp., Bedford, MA). Then they were placed on a 60-mm petri dish that contained PBS-CM and 0.2% BSA, and the solution was vigorously stirred with a small magnetic bar. Incubations were done for 3.5 h from either the apical or basolateral side with iodinated anti-HA and anti-G rabbit Fab fragments, followed by three rinses and one 2.5-h wash from both sides with the same buffer. The filters were excised with a scalpel, and their radioactivity was counted at 75% efficiency in a Packard scintillation counter (Packard Instrument Co., Inc., Downers Grove, IL). Saturation with these affinity purified antibodies was observed at 2 μg/ml (VSV) and 5 μg/ml (influenza).

Electron Microscopy

For electron microscopy, cells were plated directly on a 24-well petri dish. After the experiment was completed, they were fixed with 2% glutaraldehyde in 0.05 M sucrose, 0.1 M cacodylate buffer, pH 7.4, postfixed in 2% osmium tetroxide, and embedded directly in the petri dish. Sections were stained with uranyl acetate and lead citrate and examined in a Zeiss EM 10 electron microscope.

Stereological Measurements

Apical and basolateral surface areas were measured according to published procedures (26, 83). Briefly, the cell volume was estimated from the relationship

$$V/S = A/B,$$

in which V is volume, S is the surface of monolayer, A is the area in a given section, and B is the border of substrate section. The number of cells per surface unit was determined by counting nuclei stained with the fluorescent dye Hoechst 33258.

The membrane surface/cell volume density S_v was estimated from the relationship

$$S_v = 4/\pi\ B/A,$$

in which B is the membrane section length and A is the section area. Both lengths and areas were directly measured using a digital planimeter Microplan II (Laboratory Computer Systems, Inc., Cambridge, MA). Since the blocks were oriented so that the section was perpendicular to the substrate, the estimation of S_v was unbiased for the apical and basal plasma membrane. The measurement of the lateral domain of the plasma membrane surface was corrected as described by Sitte (78).

The virus particles observed were always closely associated with the plasma membrane. Therefore the viruses were also compared with the cell volume. The density number of particles per volume (N_v) was calculated as

$$N_v = N_a/D,$$

in which N_a is the density of viral particles per section area and D is the average caliper diameter of the viral particles. Since the geometry of the viruses is constant, VSV particles were considered as cylinders and influenza virus particles as prolate ellipsoids, and D was estimated as described by Hilliard (32).

Statistics and Calculations

The measurements are presented as mean ± standard deviation. When necessary, a Fisher's F test was applied to evaluate variance differences, and when no significant difference was found, a Student's t test was used to evaluate significance in the mean differences. To compare differences among ratios, Lexis' ratios were used to test the hypothesis of a homogeneous set of ratios versus the hypothesis of heterogeneity. The statistical significance was tested using the χ^2 distribution (35).

Results

Effect of Microtubule- and Microfilament-disrupting Agents on the Cytoskeleton of MDCK Cells

The cytoskeleton of MDCK cells has been previously described by Meza et al. (45). In monolayers extracted with 0.5% Triton X-100, the microtubular system appears as a delicate network that radiates from the nucleus (Fig. 1 *A*). Treatment with nocodazole (33 μM) or colchicine (20 μM) (Fig. 1, *C* and *D*) for 4 h resulted in complete disruption of the microtubules. Quantitation of this effect by indirect RIA (Fig. 2) indicated that 93–95% of the tubulin became extractable by detergent under these conditions. Since part of the remaining tubulin may be monomers bound to other cytoskeletal elements, it is clear that the effect of the drugs was complete. Treatment with taxol (14 μM) for 4 h resulted in typical peripheralization of microtubule bundles at the immunofluorescence level (Fig. 1 *B*) and moderate decrease of polymeric tubulin in the RIA (Fig. 2). Parallel experiments showed that, at the concentrations used, antimicrotubular drugs caused typical morphological alterations of the Golgi apparatus (49, 52, 69, 82), which was identified with anti-HA monoclonal antibody in monolayers infected with the temperature-sensitive influenza virus mutant ts61 under conditions in which most of the HA was concentrated in this organelle (67). Nocodazole and colchicine caused dispersion of the Golgi complex into multiple Golgi bodies; taxol resulted in peripheralization and compaction of the Golgi mass (data not shown). All cells in the monolayer exhibited the characteristic effect by 4 h; in fact, the effect was practically complete by 2 h. In MDCK cells, actin concentrates in stress fibers at the base of the cell and in a cortical ring (Fig. 1 *E*). Cytochalasin D (39 μM) disrupted the actin stress fibers and, after 30 min, only an image of bright cytoplasmic dots and fragmented cortical rings remained (Fig. 1 *F*). More than 90% of the cells from MDCK monolayers treated with these drug doses for 6 h were viable immediately or even 24 h later, as detected by trypan blue exclusion (not shown). This indicates that the treatment, although severe, was not lethal to the cells.

Infection with influenza virus did not affect the tubulin or actin cytoskeleton, as visualized at the immunofluorescence level with tubulin antibodies and NBD-phallacidin (data not shown). Infection with VSV caused disorganization of stress fibers and partial disruption of actin cortical rings (data not shown). However, the cytoskeleton of cells infected with influenza or VSV was still sensitive to colchicine and cytochalasin D: all microtubular structures visible in infected cells were destroyed in the presence of colchicine; treatment with cytochalasin D resulted in the appearance of fluorescent cytoplasmic actin dots (as in Fig. 1 *F*) that were not present in infected untreated cells.

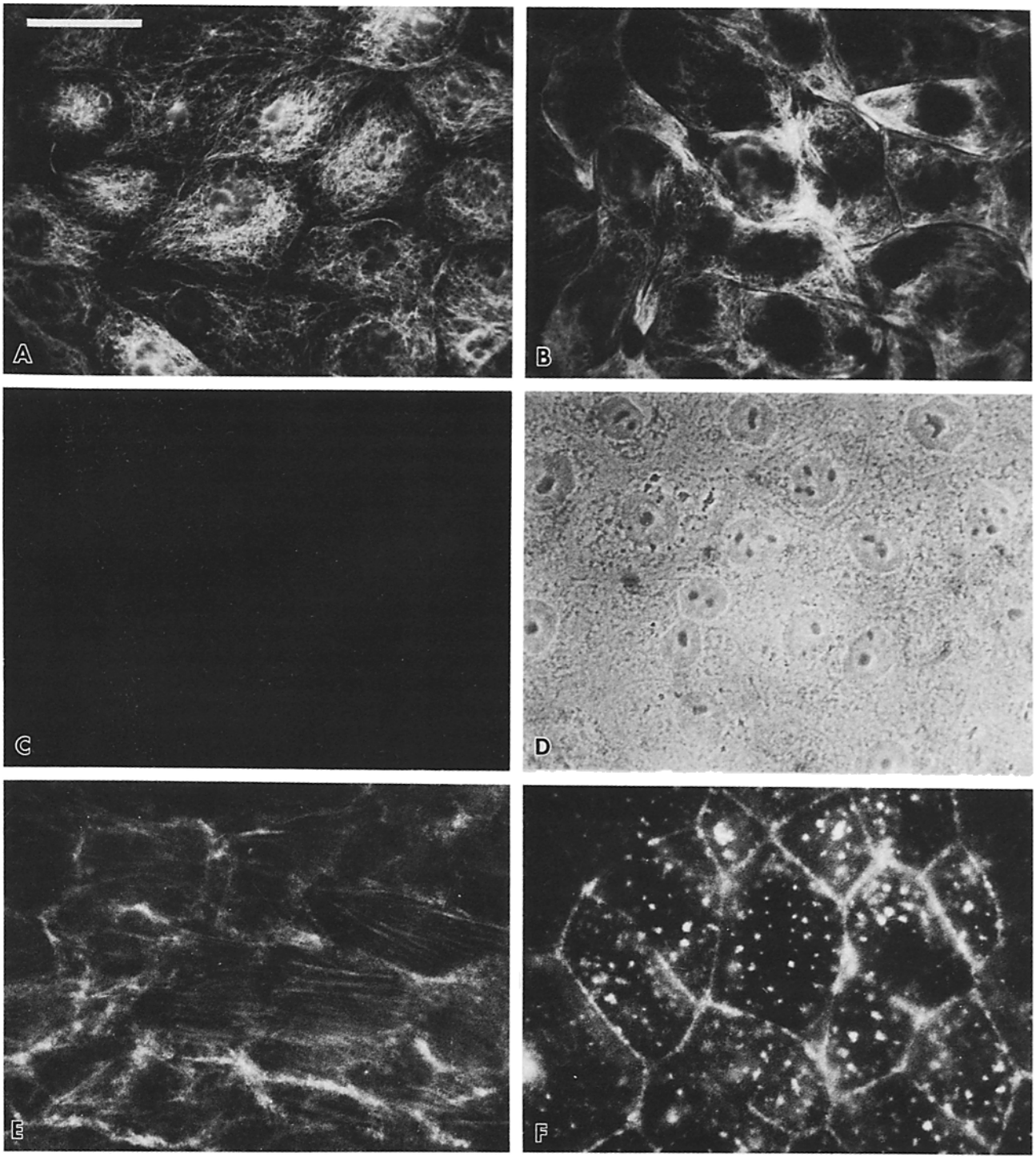

Figure 1. Effect of anticytoskeletal drugs on MDCK cells. Confluent MDCK monolayers (*A–D*), grown on glass coverslips, were treated for 4 h with 14 μM taxol (*B*), 20 μM colchicine (*C–D*), or 33 μM nocodazole (not shown), extracted for 90 s with 0.5% Triton X-100 in PHEMGT buffer, fixed with methanol for 5 min at −20°C, and processed for indirect immunofluorescence with an anti-beta-tubulin monoclonal antibody in the first step and rhodamine goat anti-mouse IgG in the second step. Identical exposure times (20 s) were used for photography of all fluorescence pictures; similar printing conditions were used for all samples. Note the dense microtubular pattern of control untreated monolayers (*A*), the typical taxol-induced disorganization of the microtubular pattern (*B*), and the complete disassembly of microtubules induced by colchicine (*C*; *D* is the corresponding phase picture). Treatment with nocodazole resulted in an image identical to *C*. (*E* and *F*) Confluent MDCK monolayers (*E*) were treated for 30 min with cytochalasin D (*F*), fixed with 2% formaldehyde, made permeable with 0.1% Triton X-100, and stained with NBD-phallacidin. Note the disappearance of the stress fibers and the concentration of actin into cytoplasmic clumps. (*E*) Control; (*F*) cytochalasin D. Bar, 10 μm.

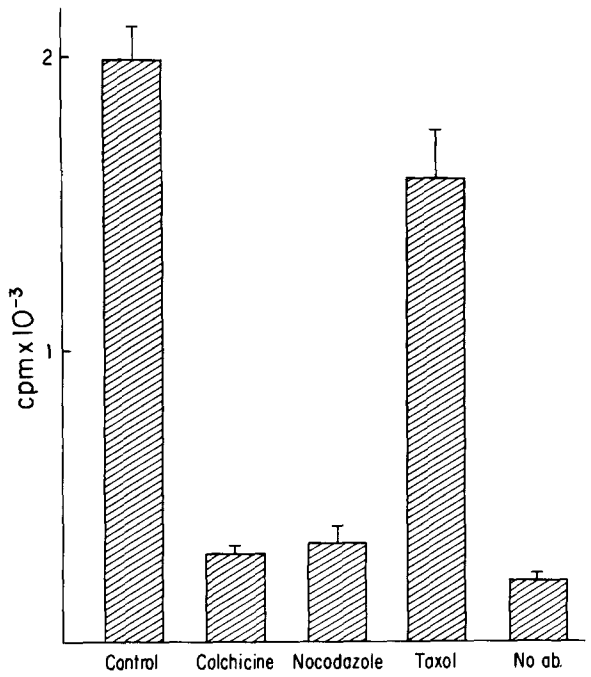

Figure 2. Determination of the extent of the effect of antimicrotubular drugs by RIA. Confluent MDCK monolayers were treated with antimicrotubular drugs (same concentrations as in legend to Fig. 1) for 4 h, treated for 90 s with 0.5% Triton X-100 in PHEMGT buffer, fixed with methanol at −20°C for 5 min, and processed for indirect RIA using a beta-tubulin monoclonal antibody in the first step and affinity purified ^{125}I-goat anti-mouse IgG in the second step. The bars represent the mean and standard deviation of quintuplicate samples (raw data, background not subtracted) processed for each drug. *No ab.*, represents the binding observed in the absence of the first antibody.

Effect of Anticytoskeletal Agents on the Polarized Budding of Influenza Virus and VSV from Confluent MDCK Monolayers

Confluent monolayers of MDCK cells were inoculated for 1 h with influenza or VSV at a moi ~10; 2 h later the experimental monolayers received medium that contained the anticytoskeletal drugs. All samples were fixed and processed for electron microscopy after 7 h of infection. Monolayers infected with VSV were covered with a 3% agarose layer after 3 h of infection, in order to trap VSV virions budding from the apical surface, and processed for electron microscopy in the presence of this layer. The polarity of viral budding was not affected by drug treatment: influenza virus preferentially budded from the apical surface (Fig. 3) and VSV from the basolateral domain (Fig. 4). The quantitative data corresponding to these experiments are shown in Tables I and II. The density of influenza virus (virions/μm^2) on the apical surface was 500–1,000 times higher than on the basolateral cell surface. Since morphometric analysis of MDCK monolayers indicate that the apical surface constitutes roughly one-fourth of the total cell surface (Table II), it follows that >99.5% of influenza virions bud from the apical cell surface; none of the drugs tested affected significantly this ratio (Table I).

VSV assembly was somewhat less polarized than influenza's. The percentage of virions budding from the apical domain ranged from 2.4 to 10.7% (Table I). Taxol and cytochalasin D resulted in somewhat reduced, although still very significant, polarity (89 and 91% basolateral, respectively). Overall, the overwhelming conclusion of these experiments is that extensive treatment of infected MDCK monolayers with anticytoskeletal drugs does not affect the asymmetric budding of apically or basolaterally budding viruses.

Table I. Polarized Assembly of Influenza and VSV from MDCK Monolayers Treated with Anticytoskeletal Drugs

Virus	Drug	Density (virions/μm^2)		Density ratio	Polarity ratio‡	*n*
		Apical	Basolateral			
		A	*B*	*B/A*	*% Apical*	
WSN	Control	10 ± 4	0.01 ± 0.05	0.001	99.7	12
	Cytochalasin D	7 ± 3	0.01 ± 0.02	0.002	99.6	11
	Colchicine	4 ± 1*	0.01 ± 0.06	0.002	99.2	10
	Nocodazole	5 ± 3*	0.01 ± 0.05	0.002	99.4	27
	Taxol	8 ± 3	0.01 ± 0.02	0.001	99.6	24
				A/B		
VSV	Control	0.3 ± 0.3	4.3 ± 2.3	0.07	2.4	18
	Cytochalasin D	0.6 ± 0.5	2.4 ± 1.0*	0.26	9.1	29
	Colchicine	0.4 ± 0.5	3.0 ± 1.5*	0.13	4.7	25
	Nocodazole	0.5 ± 0.4	4.0 ± 1.7	0.12	4.4	42
	Taxol	1.2 ± 2.1	3.9 ± 2.3	0.31	10.7	59

MDCK type II monolayers, confluent for 3–4 d, were infected with influenza virus or with VSV for 7 h, fixed, and processed for electron microscopy. Drugs were added 3 h after the start of infection. To trap VS virions released towards the apical medium, the monolayers were covered with a 3% agarose layer 3 h after VSV infection and processed for electron microscopy in the presence of this layer. Values of apical and basolateral surface areas are shown in Table II. Viral density data are expressed as mean ± SD.

* Indicates statistically significant differences with control, obtained by Student's *t* test. The statistical homogeneity of ratios was tested using Lexis' ratios and χ^2 distribution: no significant heterogeneity was found.

‡ Calculated using the formula $(A \cdot Ap/A \cdot Ap + B \cdot Bas) \cdot 100$, where *A* and *B* are the apical and basolateral viral densities (number viruses $\cdot \mu m^{-2}$), and *Ap* and *Bas* are the apical and basolateral surface areas.

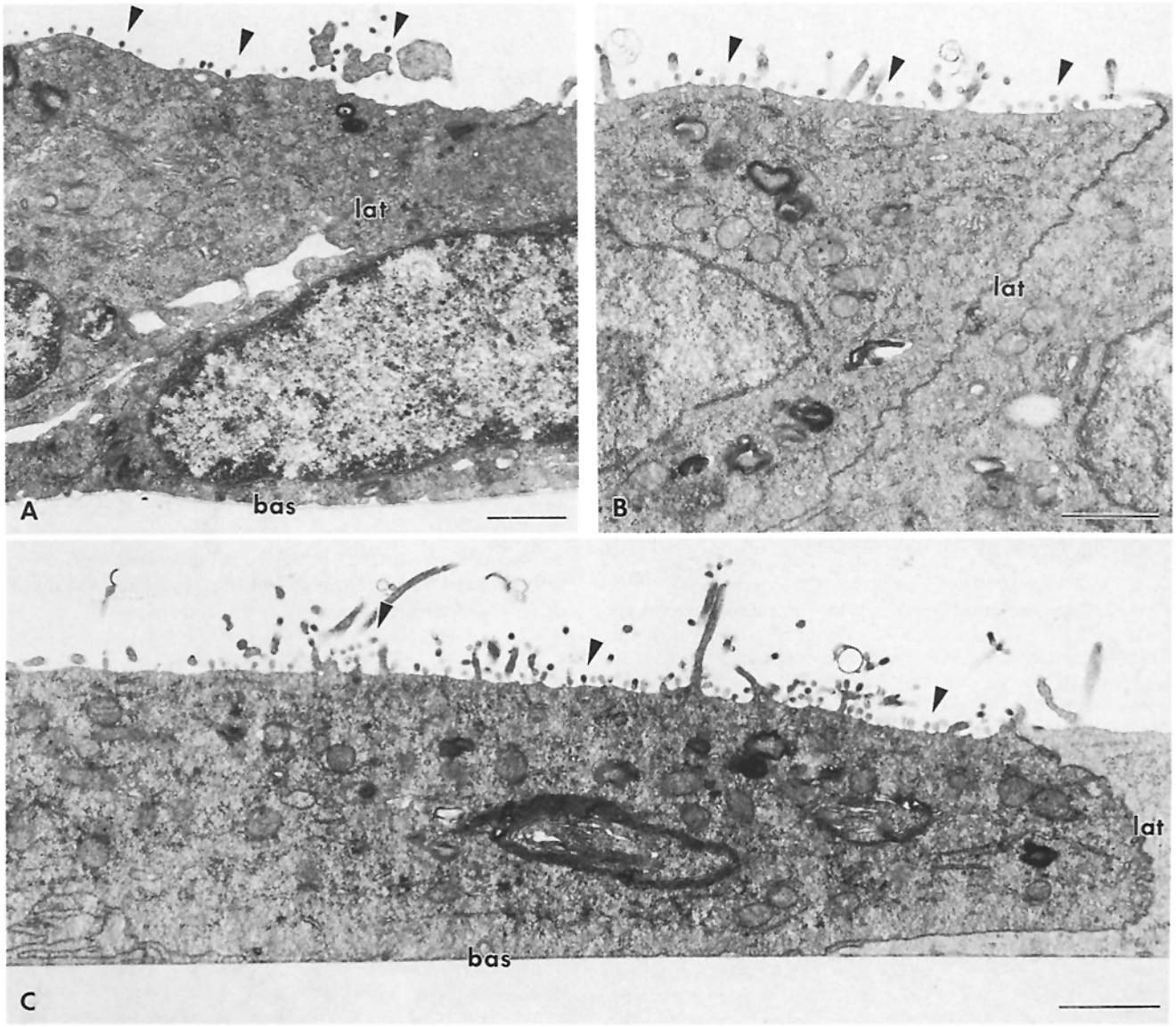

Figure 3. Polarized budding of influenza virus after disruption of the MDCK cytoskeleton. Confluent monolayers of type II MDCK cells, grown on plastic petri dishes, were inoculated with influenza virus for 1 h, exposed to anticytoskeletal drugs at 2 h, and fixed and processed for electron microscopy after 7 h of infection. Arrowheads point at virions budding from the apical surface. No virions are observed on the lateral (*lat*) or basal (*bas*) surface. (*A*) Cytochalasin D; (*B*) nocodazole; (*C*) taxol. Bars, 1 μm.

Some of the drugs used (Table I) decreased the production of influenza or VS virus up to a maximum of 50–60%. Parallel [^{35}S]methionine incorporation experiments indicated a correlation of this effect with a decreased synthesis of all viral proteins, presumably due to a toxic side effect of the drugs in MDCK cells. A previous report (22) has described no effect of 62 μM colchicine on the production of VSV by CER cells.

Effect of Anticytoskeletal Agents on the Polarized Distribution of Influenza HA and VSV G Protein

Viral budding polarity may not quantitatively be reflected in a similar degree of polarization of viral envelope glycoproteins (18). Because viral budding requires a locally very high concentration of viral envelope glycoproteins (77), it normally yields polarity ratios higher than those observed for viral envelope glycoproteins. Thus, we studied directly the effect of anticytoskeletal drugs on the surface distribution of viral glycoproteins by immunofluorescence on 0.5-μm transverse frozen sections. Strain I MDCK cells infected with TsO45 were used for experiments with VSV because G protein remains polarized for a longer time of infection than in strain II MDCK cells (reference 18 and data not shown). No dramatic changes in the polarized distributions of influenza HA and VSV G protein were detected by this procedure after treatment with antimicrotubule or antimicrofilament agents for at least 4 h (Fig. 5).

We quantitated this effect by RIA on monolayers grown on nitrocellulose filter chambers (see Materials and Methods). In a previous paper (46), it was shown that monolayers of MDCK cells grown on filters are highly impermeable to antibodies, although they allow relatively free access of macromolecules to the basolateral membrane. Table III shows

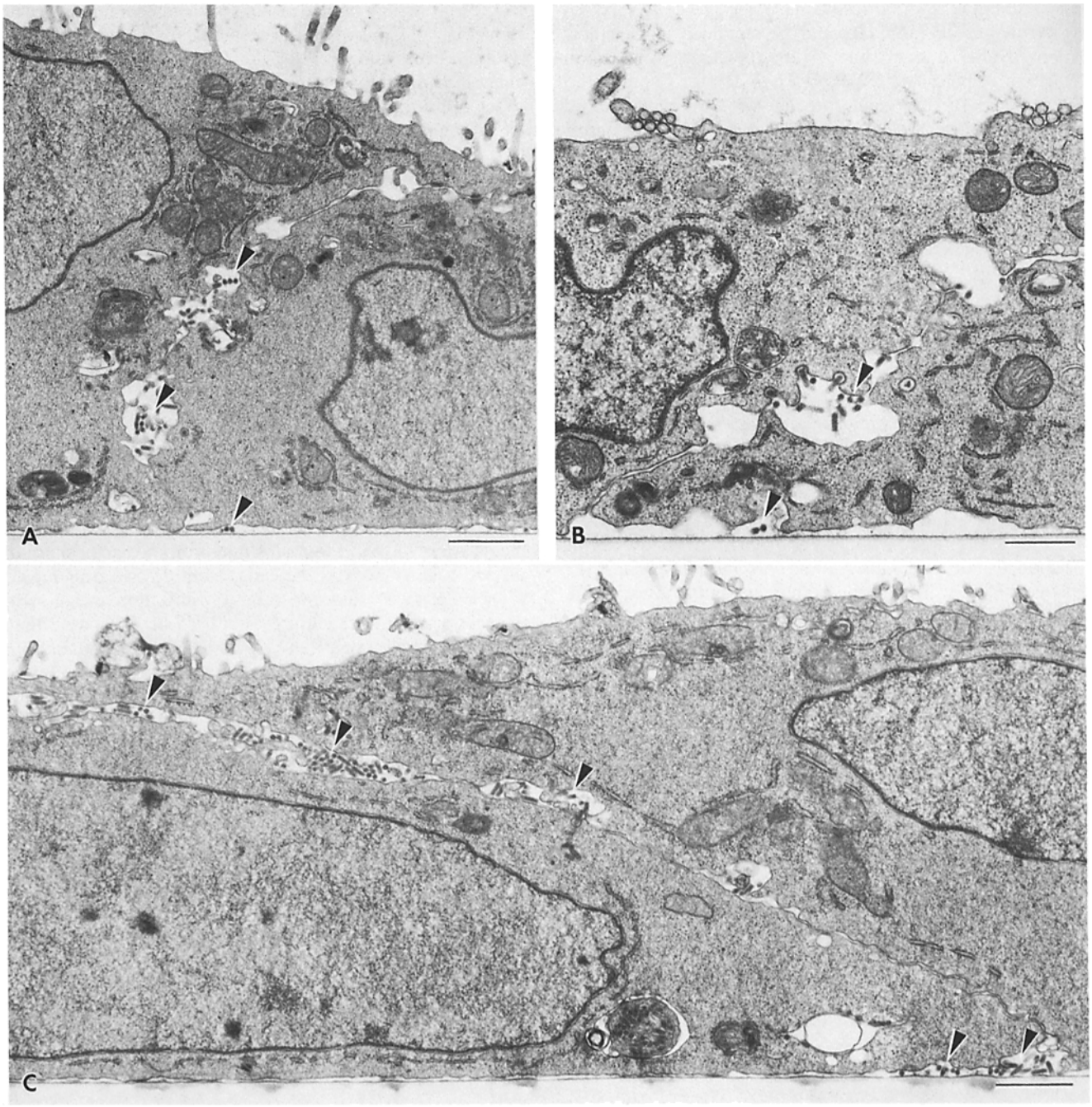

Figure 4. Polarized budding of VSV after disruption of the MDCK cytoskeleton. Confluent monolayers of type II MDCK cells, grown on plastic petri dishes, were infected with VSV and exposed to anticytoskeletal drugs as described in Fig. 2. The monolayers were covered with a layer of 3% agarose in viral growth medium at 3 h to trap virions released towards the apical medium, fixed at 7 h, and processed for electron microscopy. Note that VSV (arrowheads) is produced preferentially from the basal surface in the presence of the drugs. (*A*) Nocodazole; (*B*) cytochalasin D; (*C*) colchicine. Bars, 1 μm.

evidence that filter-grown monolayers remained tight during infection with the viruses and simultaneous treatment with the drugs. TMER of monolayers infected with influenza virus were significantly decreased by colchicine and cytochalasin D; only the latter caused a significant increase (63%) of antibody permeability. In monolayers infected with VSV, nocodazole, taxol, and cytochalasin D caused significant increases in antibody permeability (2×, 2×, and 3×, respectively) which paralleled significant decreases in TMER. Drug-treated monolayers overall remained considerable barriers to the passage of antibody molecules, as shown by the fact that cell-free filters had permeabilities at least 20 times higher (Table III). This is not surprising, since it is known that normal leaky epithelia, such as the gall bladder's, may have very low TMER (in the order of 50–100 ohms·cm^2) and still display very low permeability to macromolecules (81).

RIA experiments demonstrated a high polarization of influenza HA (~90% apical) and VSV G protein (~90% basolat-

eral) (Table IV). Similar results have been recently reported by Pfeiffer et al. (55). HA and G remained considerably polarized after 4 h treatment with the drugs. The largest reduction of polarity (to 77 and 72%) was for G protein in the presence of taxol and cytochalasin D. These reduced polarity ratios may be partially attributed to enhanced access of antibody to contralateral G protein, since these drugs caused significant increases in antibody permeability (see Table III). These experiments showed that the asymmetric distributions of influenza HA and VSV G protein were not significantly affected by microtubule- and microfilament-disrupting drugs.

Effect of Colchicine and Cytochalasin D on the Migration of Viral Glycoproteins to the Surface of MDCK Cells

The migration of influenza's HA to the cell surface was measured by RIA in confluent monolayers infected with a temperature-sensitive mutant of WSN, ts61. The temperature shift protocol used to synchronize the intracellular migration of HA has been described before (67). The cells were inoculated with ts61 and kept at the nonpermissive temperature, 40°C, for 6 h, to allow synthesis and accumulation of HA in the endoplasmic reticulum. At time 0 the monolayers infected with ts61 were shifted to the permissive temperature, 32°C, and some of them received medium with either colchicine or cytochalasin D. The shift to the permissive temperature results in the appearance of HA in the apical cell surface in 30–60 min (Fig. 6). Control and treated monolayers were fixed at different times and processed for RIA. Colchicine and cytochalasin D did not affect the kinetics of the migration of HA to the cell surface. Immunofluorescence experiments with the ts61 mutant in which the drugs were added 2 h after infection (4 h before temperature shift) did not detect any significant impairment of the migration of HA to the Golgi apparatus or to the cell surface. Identical immunofluorescence experiments with the TsO45 mutant of VSV did not detect a delay in the appearance of G protein in the Golgi apparatus or in the basolateral cell surface. Our experiments indicate that the integrity of microtubules or microfilaments is not required for the migration of viral glycoproteins from the endoplasmic reticulum to the plasma membrane of epithelial cells.

Table II. Morphometric Parameters of Infected MDCK Cells

	WSN	VSV
Cell volume (μm^3)	2,299 ± 372	2,668 ± 445
Apical surface (*Ap*) (μm^2)	1,227 ± 132	1,198 ± 93
Basolateral surface (*Bas*) (μm^2)	3,614 ± 557	3,430 ± 355
Surface area ratio (*Ap/Bas*)	0.340	0.349
% Apical surface (100 *Ap/Ap* + *Bas*)	25.4	25.9

The morphometric parameters are the averages of all measurements (drugs and controls) of experiments in Table I. Drug treatments did not induce significant variations on cell volume or membrane surface area.

Role of Microfilaments and Microtubules in the Acquisition of Epithelial Polarity

In a previous paper (66) it was shown that the polarization of viral budding is lost when the cells are incubated in suspension culture, but is recovered when the cells are plated on a substratum. To study whether microtubules and microfilaments are involved in this substrate-promoted acquisition of surface polarity, we did the experiment described in Fig. 7. MDCK cells were dissociated by trypsinization and allowed to recover in spinner culture for 12–15 h. They were then inoculated with influenza during a 1 h period, separated from free virions by centrifugation, and resuspended in the presence of colchicine or cytochalasin D. Half an hour later they were plated on plastic petri dishes (in the presence of the drugs) and, 4.5 h later, fixed with 2% glutaraldehyde for electron microscopy. Infection with influenza virus did not affect cell attachment; colchicine and cytochalasin B decreased cell attachment by 50%. Because treatment with either cytochalasin D or colchicine after infection with VSV resulted in an almost complete inhibition of cell attachment (data not shown), this experiment was done only for influenza-infected cells.

Differently from cells plated on collagen (66) only a small percentage of influenza-infected cells spread on the plastic

Table III. TMER and Antibody Permeability of MDCK Cells Infected with Influenza or VSV and Treated with Anticytoskeletal Drugs

Condition	Influenza			VSV		
	TMER		Ab leak‡	TMER		Ab leak‡
	ohms·cm²	%		*ohms·cm²*	%	
Uninfected	365 ± 18 (25)	100	ND	1,299 ± 130 (25)	100	ND
Infected	339 ± 17 (5)	93	0.038	348 ± 58 (5)	27	0.014
+ Nocodazole	297 ± 19 (5)	81	0.045	185 ± 40 (5)*	14	0.026*
+ Colchicine	246 ± 15 (5)*	67	0.046	268 ± 30 (5)	21	0.014
+ Taxol	359 ± 18 (5)	98	0.046	213 ± 34 (5)*	16	0.024*
+ Cytochalasin D	203 ± 10 (5)*	56	0.062*	66 ± 12 (5)*	5	0.040*
No cells			0.80			–

Monolayers of type II (influenza) or type I (VSV) MDCK cells, grown on nitrocellulose filter chambers for 2–3 d, were infected for 7 h with the corresponding virus and the TMER was measured by recording the voltage deflection generated by the application of 20 μA. Drugs were added 2.5 h after infection. Results are expressed as mean ± standard deviation of the mean (number of observations).

* Indicates significant differences, as determined by Student's *t* test, between control and drug-treated infected monolayers. For both viruses, infection caused a significant drop in transmonolayer resistance.

‡ Antibody leak was measured in the RIA experiments described in Table IV, but the data are presented here for comparison with the TMER. The ratio presented is cpm/ml in the apical medium per cpm/ml in the basal medium after addition of iodinated antibody (~250,000 cpm/ml) to the basal medium for 3.5 h. Only a small amount of antibody (~20× less than in the absence of cells) leaked to the apical medium, even in the presence of the drugs; however, significant increases were detected under the effect of several drugs. Note that the antibody leak was higher in type II than in type I MDCK cells.

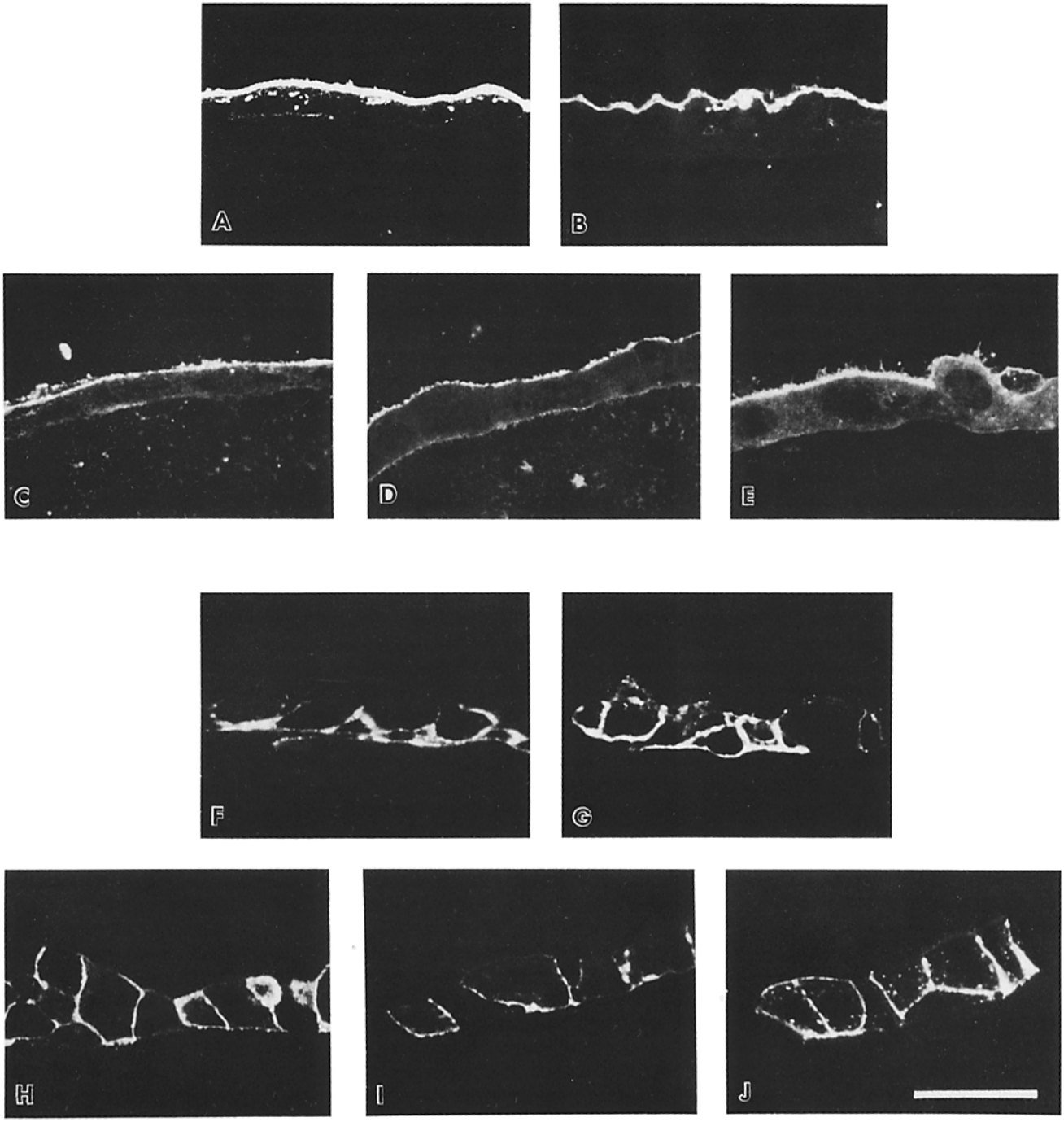

Figure 5. Asymmetric distribution of influenza HA and VSV G protein in MDCK cells treated with microfilament- and microtubule-disrupting agents. Confluent type II (*A–E*) or type I (*F–J*) MDCK monolayers grown on collagen gels were infected, respectively, with influenza virus for 6.5 h, or with VSV mutant TsO45 for 4 h at nonpermissive temperature (40°C) followed by 3 h at permissive temperature (32°C). Anticytoskeletal drugs were added after 2.5 h of infection. At the end of the incubation, the cells were fixed with 2% formaldehyde (freshly prepared from paraformaldehyde), embedded in 5% gelatin-PBS, and 0.5-μm frozen sections were processed for indirect immunofluorescence with anti-HA and anti-G antibodies (see Materials and Methods). (*A*) Influenza; (*B*) influenza + cytochalasin D; (*C*) influenza + taxol; (*D*) influenza + colchicine; (*E*) influenza + nocodazole; (*F*) VSV; (*G*) VSV + cytochalasin D; (*H*) VSV + taxol; (*I*) VSV + colchicine; (*J*) VSV + nocodazole. Colchicine and nocodazole usually increased the level of cytoplasmic fluorescence (in this case it is more obvious for nocodazole [*E*]). The basal staining observed in *D* is probably artifactual, since it is not observed on the lateral membrane. The phase image corresponding to *J* (not shown) indicates that the apparent apical label of cells 1 and 2 from the left is in fact G protein on the lateral surface, since both cells are actually covered by a cytoplasmic extension of uninfected cell 3. Bar, 10 μm.

substratum 4.5 h after plating. On the other hand, control (untreated and uninfected) cells spread very well by that time. The typical shape of infected cells is shown in Fig. 8*A*: most cells exhibited a constriction that separated an "attachment foot" from the cell body, which contained the nucleus; this constriction was absent in cytochalasin-treated cells. Budding

Table IV. Effect of Anticytoskeletal Drugs on the Asymmetric Distribution of Influenza HA and VSV G Protein, Quantitated by RIA

	Influenza		VSV	
	% Apical	% Control cpm (A + BL)	% Basolateral	% Control cpm (A + BL)
Control	90.1 ± 16.9 (5)	100	90.0 ± 21.7 (35)	100
Colchicine	80.0 ± 9.3 (5)	70	82.2 ± 17.9 (10)	85
Nocodazole	85.3 ± 19.1 (5)	74	85.7 ± 33.0 (9)	88
Taxol	88.9 ± 23.4 (5)	81	77.3 ± 11.0 (10)	109
Cytochalasin D	84.2 ± 20.8 (5)	76	72.3 ± 12.4 (5)	75

Confluent monolayers of type II MDCK cells, grown on nitrocellulose filter chambers, were infected with influenza virus for 6.5 h and processed for RIA using iodinated Fab fragments of a rabbit polyclonal against the hemagglutinin, added to the apical or to the basal medium. Drugs were added after 2.5 h of infection. For the VSV experiments, monolayers of type I (high resistance) MDCK cells were inoculated with the temperature-sensitive mutant of VSV, TsO45, at 40°C, incubated for 3 additional hours at the same temperature, and then transferred for 3 h to 32°C, the permissive temperature. Drugs were added 2 h before the temperature shift so that the total time of treatment was 5 h. RIA was done using iodinated Fab fragments of a rabbit antibody against G protein. Results are expressed as mean ± standard deviation of the mean (number of observations). None of the differences were found to be significant by Student's *t* test. The total cpm (apical + basolateral [A + BL]) of control samples was 11,374 for influenza and 5,061 for VSV, after background subtraction. Background radioactivity bound to uninfected samples was, for influenza, 2,200 (apical) and 2,100 cpm (basolateral) and for VSV, 1,140 (apical) and 1,095 cpm (basolateral).

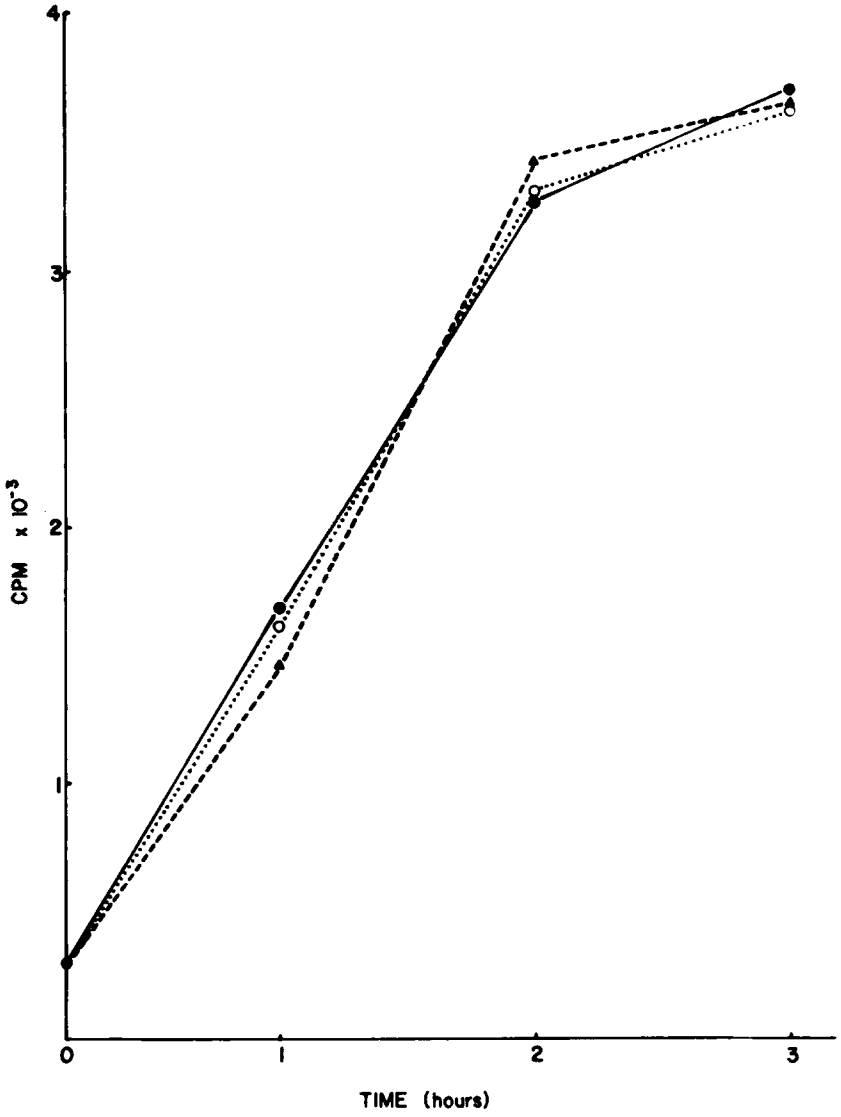

Figure 6. Effect of colchicine and cytochalasin D on the kinetics of influenza's HA migration to the cell surface. Confluent MDCK monolayers grown on 50-well tissue culture dishes (detachable wells) were infected with Ts61 and incubated for 6 h at the nonpermissive temperature (40°C) so that viral HA was produced but arrested at the endoplasmic reticulum. At time 0 the cells were shifted to the permissive temperature (32°C) in the presence of colchicine (20 μM) or cytochalasin D (39 μM). Quintuplicate monolayers were fixed at 0, 1, 2, and 3 h after shift and processed for indirect RIA with a monoclonal antibody against HA followed by ^{125}I-goat anti-mouse IgG. Individual wells (~8×10^4 cells) were detached and counted separately. Standard deviations were <10% of the mean values. ●, control; ○, colchicine; ▲, cytochalasin D.

of influenza virions occurred preferentially from the free surface, particularly from the cell body: few virions were observed either on the free or the attached surfaces of the "foot" (Fig. 8, *A–C*). Colchicine (Fig. 8, *D–F*) or cytochalasin D (data not shown) did not alter this polarity. BHK cells, of fibroblastic lineage, exhibited a strikingly different behavior when infected with influenza virus and plated on the substrate; many influenza virions were observed budding from the attached surface (Fig. 8 *G*).

Quantitative data obtained from the analysis of these ex-

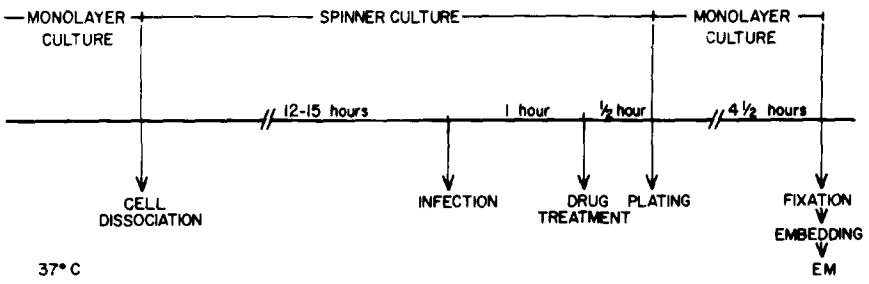

Figure 7. Protocol for infection of MDCK cells in suspension culture.

periments are shown in Table V. The ratio free/attached surface section was inverted with respect to the one observed in confluent monolayers: the free surface sectional lengths were 80%, 89%, and 87% of the total sectional surface length, respectively, for control, cytochalasin D, and colchicine-treated cells. The asymmetry of the budding was estimated from the ratio *A/F*: number of virions per micrometer of attached membrane section/number of virions per micrometer of free surface. This ratio turned out to be strikingly different in epithelial (MDCK) and fibroblastic (BHK) cells. The high *A/F* ratio observed in BHK cells, although somewhat artificial because many of the virions counted in the basal area were trapped virions, highlights the ability of MDCK cells to exclude influenza virus budding from the attached surface. The failure of both colchicine and cytochalasin D to abolish the acquisition of virus budding polarity indicates that microfilaments and microtubules sensitive to the action of these drugs are not involved in this process. Rather, the development of polarity upon contact with the substrate, at least regarding the mechanisms involved in the polarized budding of an apical virus, appears to be a cell surface phenomenon.

Discussion

Microtubules and Actin Filaments Are Not Responsible for Polarized Viral Budding

The results of this report indicate that microtubules and microfilaments are not critically involved in the maintenance of polarity in confluent monolayers of MDCK cells. The effect of anti-microtubular agents was found to be complete. The action of cytochalasin D was less complete, however: although microvilli and stress fibers disappeared, a fragmented actin ring still remained at the level of the tight and adherent junctions.

Although the drugs were fully effective in 1–2 h, the budding of influenza and VSV viruses from the surface of MDCK cells 5 h after drug addition, carefully quantitated by morphometric procedures, was found to remain highly polar (under these conditions, some of the drugs reduced the surface density of influenza and VS virions by up to 60%; most of this effect could be attributed to a decrease in viral protein synthesis). Influenza was found to be the most polarized of the two viruses studied: 99.7% of the virions budded from the apical surface, which constitutes only one-fourth of the total surface area of confluent type II MDCK cells. None of the drugs decreased significantly this proportion. The polarity of VSV budding was lower: virions on the "incorrect" surface were 20–50 out of 1,000 as compared with influenza's 3–5. Since the basolateral surface area constitutes about three-fourths of the total surface area, this result suggests that more strict polarization mechanisms operate for apical than for basolateral viruses. As with influenza virus, anticytoskeletal agents did not affect significantly the polarity of virus budding: only taxol and cytochalasin D decreased slightly the percentage of basolateral VSV. Thus, the maintenance of polarity by epithelial cells is not affected (or only marginally affected) by anticytoskeletal agents, at least regarding their ability to sustain polarized viral budding.

Actin Filaments and Microtubules Are Not Critically Involved in the Intracellular Transport and Asymmetric Distribution of Influenza HA and VSV G Protein

Frozen sections of MDCK monolayers grown on collagen gels allowed direct and unequivocal visualization of influenza HA and VSV G protein in the apical and basolateral surface. Both glycoproteins appeared highly polarized by this procedure and none of the drugs used appeared to alter significantly their polarized distribution. This was confirmed by using quantitative RIA on monolayers grown on filters: 90% of the HA and G protein were found, respectively, on the apical and basolateral surface. Only cytochalasin D and taxol caused a small decrease in the polarization of VSV G protein; these effects might be partially artifactual due to opening of some tight junctions (and enhanced access of lateral antigen to antibody in the apical medium) under the combined influence of the drug and the infection with VSV. The intracellular transport of influenza HA and VSV G protein was not affected, either, by colchicine or cytochalasin D. Therefore, it seems that, differently from regulated secretory proteins, viral glycoprotein transport and, by extension, plasma membrane protein transport does not depend on the presence of a complete actin/tubulin cytoskeleton. This discrepancy might be explained if microtubule participation in secretory events occurs at segments of the secretory pathway not shared by constitutive plasma membrane proteins. In fact, while it has been shown that there is overlap between the pathways of secretory and plasma membrane proteins at the levels of the endoplasmic reticulum and Golgi apparatus (80), viral envelope glycoproteins and proteins subject to regulated secretion appear to be transported by different post Golgi vesicles (24, 28, 48).

Vectorial Exocytosis of Vesicles That Transport Apical and Basolateral Glycoproteins May Require Domain-specific "Docking" Receptors

It is clear now that the sorting of apical and basolateral viral glycoproteins is an intracellular event occurring at a late Golgi or post Golgi stage. An acid phosphatase–positive *trans* Golgi tubulocisternal network, where transport of viral glycoproteins is delayed by incubation at 20°C, appears to be a good

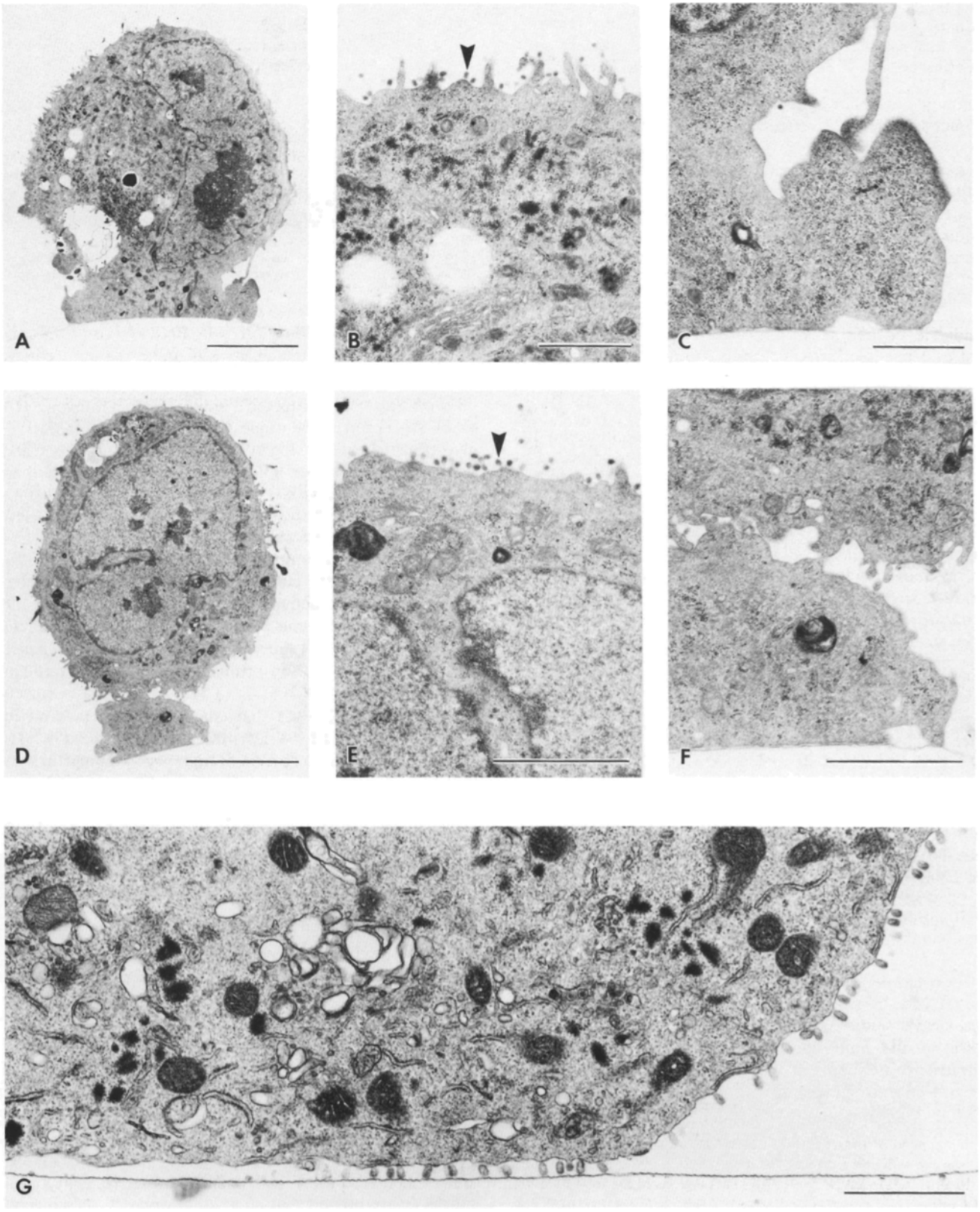
A
B
C
D
E
F
G

Table V. Effect of Cytochalasin D and Colchicine on the Budding of Influenza Virus from Subconfluent MDCK and BHK Cells Plated 4.5 H Earlier

Drug	Membrane section (μm)		Virions/10-μm section			
	Free surface	Attached surface	Free surface	Attached surface	*A/F*	*n*
MDCK cells						
Control	56 ± 16	14 ± 7	9.1 ± 8	2.0 ± 3	0.25	22
Cytochalasin D	63 ± 13	8 ± 5	6.7 ± 2	0.6 ± 1	0.07	7
Colchicine	68 ± 23	10 ± 3	9.7 ± 6	0.7 ± 1	0.08	16
BHK cells						
Control	52 ± 33	23 ± 13	0.2 ± 0.3	5.0 ± 3	32.0	11

MDCK and BHK cells were dissociated from confluent monolayers by treatment with trypsin EDTA and kept in suspension culture for 10–12 h. The following day, they were inoculated with influenza virus for 1 h, treated with cytochalasin D or colchicine, and plated 30 min later in the presence of the drugs at subconfluent levels. 4.5 h later the subconfluent monolayers were fixed and processed for electron microscopy. For quantitation purposes, the plasma membrane of MDCK and BHK cells was morphologically divided into attached and free surface. Although the free surface of the attachment foot shares some of the properties of the attached surface (lack of microvilli and decreased density of budding virions), we have included it in the free surface for statistical purposes, because the boundary of the attachment foot is not as well defined as the boundary between attached and free surfaces.

* Note that *A/F*, the ratio of virus number per micrometer of attached surface section (*A*)/virus number per micrometer of free surface section (*F*), is very different for MDCK or BHK cells. Lexis' ratios indicated no significant heterogeneity among *A/F* ratios for MDCK cells, but a very significant heterogeneity when the ratio for BHK cells was included ($P < 0.01$). This shows that *A/F* is a measurement of a property of epithelial cells.

candidate for the sorting compartment (27, 42, 44, 55). Current evidence (see Introduction) is compatible with a model in which specific carrier vesicles transport apical and basolateral glycoproteins from the sorting compartment to the respective surface domain. Our results suggest that, while microtubules and special dynein-like microtubule associated proteins may be involved in fast intracellular transport processes (1, 74), including regulated secretion, they do not provide specific "tracks" for the slower biogenetic transport of vesicles that carry apical or basolateral plasma membrane glycoproteins. It may be speculated that vesicles involved in the latter process move randomly in the cytoplasm and are "captured" by specific "docking receptors" in the respective surface. Rothman and his colleagues (15) have recently presented evidence for a similar receptor-mediated vesicular mechanism that operates in the transport of VSV G protein between different Golgi subcompartments.

Role of the Substrate and the Submembrane Cytoskeleton in the Development of Epithelial Polarity

Previous experiments have indicated a crucial role for the substrate in the development of surface polarity in epithelial cells (66). We have now shown that MDCK cells can develop the ability to sustain polarized budding of influenza virus upon attachment to the substrate even in the presence of antimicrotubule or antimicrofilament agents. On the other hand, a fibroblastic kidney cell line, BHK, failed to develop polarized budding of influenza virus under the same conditions, in the absence of the drugs. It is tempting to speculate that this represents a fundamental difference between epithelial cells and fibroblasts. More work is needed to clarify this point, however, since Brown and Salomonsky (7) have shown some qualitative evidence that influenza virus budding may be asymmetric in L cells (fibroblasts). The experiments in this report indicate that actin filaments and microtubules are not essential for the substrate-dependent surface polarization of epithelial cells. At this time, the possible role of other cytoskeleton components, such as myosin or intermediate filaments, or spectrin-like molecules tightly associated to the cytoplasmic aspect of the plasma membrane, cannot be excluded. There is, in fact, some evidence that these molecules may show polarity in other epithelia and in the early embryo (14, 20, 54, 79).

Our results suggest that the establishment of polarity in epithelial cells, as determined from the polarized viral budding, is mainly a cell surface event triggered by the attachment to the substrate. This process appears to have several stages, the initial one might be the recruitment of just a restricted set of plasma membrane proteins in the attached surface (for example, receptors for collagen or laminin, see reference 72). This may be sufficient to determine the polarization of some surface molecules, for example those involved in the asymmetric budding of viruses, but may not be enough to support

Figure 8. Acquisition of asymmetric influenza virus budding by isolated MDCK cells after attachment to the substrate in the presence of colchicine. MDCK cells were dissociated with trypsin-EDTA, incubated overnight in spinner culture, infected with influenza virus, and plated on plastic petri dishes 1.5 h after infection. Colchicine (20 μM) was added after 1 h of infection. 4.5 h after plating (i.e., after 6 h of infection), the cells were fixed and processed for electron microscopy. (*A–C*) Control cell; (*B*) detail of the free surface of the same cell; (*C*) detail of the free and attached surfaces of the attachment foot; (*D–F*) colchicine treated; (*E*) detail of the free surface of the same cell; (*F*) detail of the free and attached surfaces of the attachment foot; (*G*) BHK (fibroblastic cell) processed using the same protocol. Most of the infected MDCK cells (either treated or untreated) do not spread on the plastic substratum 4.5 h after plating, while uninfected cells do (not shown). Infected cells show microvilli and a typical "attachment foot." Note that most of the influenza viruses bud from the free surface of the cell body; practically no virions bud from the free or attached regions of the foot. Quantitative data are shown in Table V. Bars: (*A* and *D*) 10 μm; (*B, C, D, F,* and *G*) 1 μm.

the polarization of other markers, such as the basolateral MDCK antigens studied by Balcarova-Stander et al. (3) and by Herzlinger and Ojakian (31). Recent evidence (Vega-Salas, D. E., D. Gundersen, P. J. I. Salas, and E. Rodriguez-Boulan, manuscript submitted for publication) indicates that two apical markers of MDCK cells are polarized in monolayers without functional tight junctions but two basolateral markers are not. Current work in our laboratory is directed to understanding how cell–substrate and cell–cell interactions trigger the development of polarity in epithelial cells.

We thank Drs. Donald Fischman, Peter Sherline, and Joel Pardee for helpful discussions of the manuscript and advice on quantitation of polymerized tubulin, Ms. Anne Bushnell and Mr. James Dennis for excellent technical assistance with the electron microscopy, and Ms. Lori van Houten for skillful photographic work.

This work was supported by grants from National Institutes of Health (GM 34107 and AM 26481) and National Science Foundation (PCM-8217405). P. J. I. Salas was recipient of a Fogarty International Fellowship. E. Rodriguez-Boulan was recipient of a career award from the Irma T. Hirschl Trust and an Established Investigator award from the American Heart Association.

Received for publication 3 November 1985, and in revised form 29 January 1986.

References

1. Allen, R. D., D. T. Brown, S. P. Gilbert, and H. Fujiwake. 1983. Transport of vesicles along filaments dissociated from squid axoplasm. *Biol. Bull.* 165:523.

2. Andrews, P. M. 1981. Investigations of cytoplasmic contractile and cytoskeletal elements in the kidney glomerulus. *Kidney Int.* 20:549–562.

3. Balcarova-Stander, J., S. E. Pfeiffer, S. D. Fuller, and K. Simons. 1984. Development of cell surface polarity in the epithelial Madin-Darby canine kidney (MDCK) cell line. *EMBO (Eur. Mol. Biol. Organ.) J.* 3:2687–2694.

4. Bauduin, H., C. Stock, D. Vincent, and F. Grenier. 1975. Microfilamentous system and secretion of enzyme in the exocrine pancreas. Effect of cytochalasin B. *J. Cell Biol.* 66:165–181.

5. Blose, S. H., D. I. Meltzer, and J. R. Feramisco. 1984. 10 nm filaments are induced to collapse in living cells microinjected with monoclonal and polyclonal antibodies against tubulin. *J. Cell Biol.* 98:847–858.

6. Bretscher, A. P., and K. Weber. 1978. Localization of actin and microfilament associated proteins in the microvilli and terminal web of the intestinal brush border by immunofluorescence microscopy. *J. Cell Biol.* 79:839–845.

7. Brown, J. C., and N. L. Salomonsky. 1985. Site-specific maturation of enveloped viruses in L cells treated with cytochalasin B. *J. Cell Biol.* 100:357–363.

8. Busson-Mabillot, S., A.-M. Chambaut-Guerin, L. Ovtracht, P. Muller, and B. Rossignol. 1982. Microtubules and protein secretion in rat lacrimal glands: localization of short-term effects of colchicine on the secretory process. *J. Cell Biol.* 95:105–117.

9. Cereijido, M., E. S. Robbins, W. J. Dolan, C. A. Rotunno, and D. Sabatini. 1978. Polarized monolayers formed by epithelial cells on a permeable and translucent support. *J. Cell Biol.* 77:853–880.

10. Cereijido, M., E. Rodriguez-Boulan, L. Borboa, A. Gonzalez-Robles, and G. Beaty. 1983. The relationship between occluding junctions and polarity in epithelioid cells (MDCK). *J. Cell Biol.* 97 (5, Pt. 2):80a. (Abstr.)

11. Cho, M. I., and P. R. Garant. 1981. Role of microtubules in the organization of the Golgi complex and the secretion of collagen secretory granules by periodontal ligament fibroblasts. *Anat. Rec.* 199:459–471.

12. Craig, W. S., and J. V. Pardo. 1979. Alpha-actinin localization in the junctional complex of intestinal epithelial cells. *J. Cell Biol.* 80:203–210.

13. Diegerman, R. F., and B. Peterkofsky. 1972. Inhibition of collagen secretion from bone and cultured fibroblasts by microtubular disruptive drugs. *Proc. Natl. Acad. Sci. USA.* 69:892–896.

14. Drenckhahn, D., K. Schluter, D. P. Allen, and V. Bennett. 1985. Colocalization of Band 3 with ankyrin and spectrin at the basal membrane of intercalated cells in the rat kidney. *Science (Wash. DC).* 230:1287–1289.

15. Dunphy, W. G., and J. E. Rothman. 1985. Compartmental organization of the Golgi stack. *Cell.* 42:13–21.

16. Ehrlich, H. P., R. Ross, and P. Bornstein. 1974. Effects of antimicrotubular agents on the secretion of collagen. A biochemical and morphological study. *J. Cell Biol.* 62:390–405.

17. Farquhar, M., and G. Palade. 1963. Junctional complexes in various epithelia. *J. Cell Biol.* 17:375–412.

18. Fuller, S. D., C.-H. von Bonsdorff, and K. Simons. 1984. Vesicular stomatitis virus infects and matures only through the basolateral surface of the polarized epithelial cell line MDCK. *Cell.* 38:65–77.

19. Fuller, S. D., R. Bravo, and K. Simons. 1985. An enzymatic assay reveals that proteins destined for the apical or basolateral domains of an epithelial cell line share the same Golgi compartments. *EMBO (Eur. Mol. Biol. Organ.) J.* 4:297–307.

20. Geiger, B., K. T. Tokuyasu, A. H. Dutton, and S. J. Singer. 1980. Vinculin, an intracellular protein localized at specialized sites where microfilament bundles terminate at cell membranes. *Proc. Natl. Acad. Sci. USA.* 77:4127–4131.

21. Geiger, B., K. T. Tokuyasu, and S. J. Singer. 1979. Immunocytochemical localization of alpha-actinin in intestinal epithelial cells. *Proc. Natl. Acad. Sci. USA.* 76:2833–2837.

22. Genty, N., and F. Bussereau. 1980. Is cytoskeleton involved in vesicular stomatitis virus reproduction? *J. Virol.* 34:777–781.

23. Goodenough, D. A., and J. P. Revel. 1970. A fine structural analysis of intercellular junctions in the mouse liver. *J. Cell Biol.* 45:272–290.

24. Green, R., and D. Shields. 1984. Somatostatin discriminates between the intracellular pathways of secretory and membrane proteins. *J. Cell Biol.* 99:97–104.

25. Griffin, J. A., and R. W. Compans. 1979. Effect of cytochalasin B on the maturation of enveloped viruses. *J. Exp. Med.* 150:379–391.

26. Griffiths, G., G. Warren, P. Quinn, O. Mathieu-Costello, and H. Hoppeler. 1984. Density of newly synthesized plasma membrane proteins in intracellular membranes. I. Stereological studies. *J. Cell Biol.* 98:2133–2141.

27. Griffiths, G., S. Pfeiffer, K. Simons, and K. Matlin. 1985. Exit of newly synthesized membrane proteins from the trans cisterna of the Golgi complex to the plasma membrane. *J. Cell Biol.* 101:949–964.

28. Gumbiner, B., and R. B. Kelly. 1982. Two distinct intracellular pathways transport secretory and membrane glycoproteins to the surface of pituitary tumor cells. *Cell.* 28:51–59.

29. Handler, J. S., F. M. Perkins, and J. P. Johnson. 1980. Studies of renal function using cell culture techniques. *Am. J. Physiol.* 238:F1–F9.

30. Hayden, J. H., R. D. Allen, and R. D. Goldman. 1983. Cytoplasmic transport in keratocytes: direct visualization of particle translocation along microtubules. *Cell Motil.* 3:1–19.

31. Herzlinger, D. A., and G. Ojakian. 1984. Studies on the development and maintenance of epithelial cell surface polarity with monoclonal antibodies. *J. Cell Biol.* 98:1777–1787.

32. Hilliard, J. E. 1967. The calculation of the mean caliper diameter of a body for use in the analysis of the number of particles per unit volume. *In* Stereology. H. Elias, editor. Springer-Verlag, Berlin. 211–215.

33. Howell, S. L., and M. Tyhurst. 1978. Role of microtubules in the intracellular transport of growth hormone. *Cell Tissue Res.* 190:163–171.

34. Kemper, B., J. F. Habener, A. Rich, and J. P. Potts. 1975. Microtubules and the intracellular conversion of proparathyroid hormone to parathyroid hormone. *Endocrinology.* 96:903–912.

35. Kendall, M. G. 1952. The Advanced Theory of Statistics. Volume 2. Ch. Griffin & Co., Ltd., London. 119–122.

36. Knapp, L. W., W. M. O'Guin, and R. H. Sawyer. 1983. Drug induced alterations of cytokeratin organization in cultured epithelial cells. *Science (Wash. DC).* 219:501–503.

37. Leighton, J., Z. Brada, L. W. Estes, and G. Justh. 1969. Secretory activity and oncogenicity of a cell line derived from canine kidney. *Science (Wash. DC).* 162:472–473.

38. Lodish, H. F., W. A. Braell, A. L. Schwartz, G. J. A. M. Strous, and A. Zilberstein. 1981. Synthesis and assembly of membrane and organelle proteins. *Int. Rev. Cytol.* 12(Suppl):247–307.

39. Louvard, D. 1980. Apical membrane aminopeptidase appears at site of cell-cell contact in cultured kidney epithelial cells. *Proc. Natl. Acad. Sci. USA.* 77:4132–4136.

40. Madara, J. L. 1983. Increases in guinea pig small intestinal transepithelial resistance induced by osmotic loads are accompanied by rapid alterations in absorptive-cell tight junction structure. *J. Cell Biol.* 97:125–136.

41. Malaisse-Lagae, F., M. Amherdt, M. Ravazzola, A. Sener, J. C. Hutton, L. Orci, and W. J. Malaisse. 1979. Role of microtubules in the synthesis, conversion and release of proinsulin. A biochemical and radioautographic study in rat islets. *J. Clin. Invest.* 63:1284–1296.

42. Matlin, K. S., and K. Simons. 1983. Reduced temperature prevents transfer of a membrane glycoprotein to the cell surface but does not prevent terminal glycosylation. *Cell.* 34:233–243.

43. Matlin, K. S., D. Bainton, M. Pesonen, N. Genty, D. Louvard, and K. Simons. 1983. Transfer of a viral envelope glycoprotein from the apical to the basolateral plasma membrane of MDCK cells. I. Morphological evidence. *J. Cell Biol.* 97:627–637.

44. Matlin, K. S., and K. Simons. 1984. Sorting of an apical plasma membrane glycoprotein occurs before it reaches the cell surface in cultured epithelial cells. *J. Cell Biol.* 99:2131–2139.

45. Meza, I., G. Ibarra, M. Sabanero, A. Martinez-Palomo, and M. Cereijido. 1980. Occluding junctions and cytoskeletal components in a cultured transporting epithelium. *J. Cell Biol.* 87:746–754.

46. Misek, D. E., E. Bard, and E. Rodriguez-Boulan. 1984. Biogenesis of epithelial cell polarity: intracellular sorting and vectorial exocytosis of an apical plasma membrane glycoprotein. *Cell.* 39:537–546.

47. Misfeldt, D. S., S. T. Hamamoto, and D. R. Pitelka. 1976. Transepithelial transport in cell culture. *Proc. Natl. Acad. Sci. USA.* 73:1212–1216.

48. Moore, H. P., B. Gumbiner, and R. B. Kelly. 1983. Chloroquine diverts ACTH from a regulated to a constitutive secretory pathway in atT-20 cells. *Nature (Lond.).* 302:434–436.

49. Moskalewski, S., J. Thyberg, S. Lohmander, and U. Friberg. 1975. Influence of colchicine and vinblastine on the Golgi complex and matrix deposition in chondrocyte aggregates. *Exp. Cell Res.* 95:440–454.

50. Ojakian, G. K. 1981. Tumor promoter-induced changes in the permeability of epithelial cell tight junctions. *Cell.* 23:95–103.

51. Ollivier-Bousquet, M., and R. Denamur. 1973. Inhibition par la colchicine de la secretion des proteines du lait. *C. R. H. Acad. Sci. (Paris) Ser. D.* 276:2183–2186.

52. Pavelka, M., and A. Ellinger. 1983. Effect of colchicine on the Golgi complex of rat pancreatic acinar cells. *J. Cell Biol.* 97:737–748.

53. Patzelt, C., D. Brown, and B. Jeanrenaud. 1977. Inhibitory effect of amylase secretion by rat parotid glands. Possible localization in the Golgi area. *J. Cell Biol.* 73:578–593.

54. Philp, N. J., and V. T. Nachmias. 1985. Components of the cytoskeleton in the retinal pigmented epithelium of the chick. *J. Cell Biol.* 101:358–362.

55. Pfeiffer, S., S. D. Fuller, and K. Simons. 1985. Intracellular sorting and basolateral appearance of the G protein of vesicular stomatitis virus in Madin-Darby canine kidney cells. *J. Cell Biol.* 101:470–476.

56. Quaroni, A., K. Kirsch, and M. M. Weisen. 1979. Synthesis of membrane glycoproteins in rat small intestinal villus cells. Effect of colchicine on the redistribution of L-[1,5,6-^{3}H]fucose-labelled membrane glycoproteins among Golgi, lateral basal and microvillus membranes. *Biochem. J.* 182:213–221.

57. Radke, K., V. C. Carter, P. Moss, P. Dehazya, M. Schliwa, and G. S. Martin. 1983. Membrane association of a 36,000 dalton substrate for tyrosine phosphorylation in chicken embryo fibroblasts transformed by avian sarcoma viruses. *J. Cell Biol.* 97:1601–1611.

58. Redman, C. M., D. Banerjee, K. Howell, and G. E. Palade. 1975. Colchicine inhibition of plasma protein release from rat hepatocytes. *J. Cell Biol.* 66:42–59.

59. Richardson, J. C. W., V. Scalera, and N. L. Simmons. 1981. Identification of two strains of MDCK cells which resemble separate nephron tubule segments. *Biochim. Biophys. Acta.* 673:26–36.

60. Rindler, M. J., I. E. Ivanov, E. Rodriguez-Boulan, and D. Sabatini. 1982. Biogenesis of epithelial cell plasma membranes. *In* Membrane Recycling. D. Collins, editor. Ciba Foundation Symposium 92. Putnam, London. 184–202.

61. Rindler, M. J., I. E. Ivanov, H. Plesken, E. Rodriguez-Boulan, and D. Sabatini. 1984. Viral glycoproteins destined for apical or basolateral domains traverse the same Golgi apparatus during their intracellular transport in doubly infected Madin-Darby canine kidney cells. *J. Cell Biol.* 98:1304–1319.

62. Rindler, M. J., I. E. Ivanov, H. Plesken, and D. D. Sabatini. 1985. Polarized delivery of viral glycoproteins to the apical and basolateral plasma membranes of MDCK cells infected with temperature sensitive viruses. *J. Cell Biol.* 100:136–151.

63. Rodriguez-Boulan, E. 1983. Membrane biogenesis, enveloped RNA viruses and epithelial polarity. *Mod. Cell Biol.* 1:119–170.

64. Rodriguez-Boulan E. 1983. Polarized budding of viruses from epithelial cells. *Methods Enzymol.* 98:486–501.

65. Rodriguez-Boulan, E., and M. Pendergast. 1980. Polarized distribution of viral envelope proteins in the plasma membrane of infected epithelial cells. *Cell.* 20:45–54.

66. Rodriguez-Boulan, E., K. Paskiet, and D. Sabatini. 1983. Assembly of enveloped viruses in Madin-Darby canine kidney cells: polarized budding from single attached cells and from clusters of cells in suspension. *J. Cell Biol.* 96:866–874.

67. Rodriguez-Boulan, E., K. Paskiet, P. J. I. Salas, and E. Bard. 1984. Intracellular transport of influenza virus hemagglutinin to the apical surface of Madin-Darby canine kidney cells. *J. Cell Biol.* 98:308–319.

68. Rodriguez-Boulan, E., and D. Sabatini. 1978. Asymmetric budding of viruses in epithelial monolayers: a model system for study of epithelial polarity. *Proc. Natl. Acad. Sci. USA.* 75:5071–5075.

69. Rogalski, A. A., and S. J. Singer. 1984. Associations of elements of the Golgi apparatus with microtubules. *J. Cell Biol.* 99:1092–1100.

70. Rogalski, A. A., J. E. Bergman, and S. J. Singer. 1984. Effect of microtubule assembly status on the intracellular processing and surface expression of an integral protein of the plasmam membrane. *J. Cell Biol.* 99:1101–1109.

71. Sabatini, D. D., G. Kreibich, T. Morimoto, and M. Adesnik. 1982. Mechanisms for incorporation of proteins in membranes and organelles. *J. Cell Biol.* 92:1–22.

72. Salas, P. J. I., D. Vega-Salas, D. Misek, and E. Rodriguez-Boulan. 1985. Intracellular routes of apical and basolateral plasma membrane proteins to the surface of epithelial cells. *Pfluegers Arch. Eur. J. Physiol.* 405:S152–S157.

73. Schliwa, M. 1984. Mechanisms of intracellular organelle transport. *In* Cell and Muscle Motility. Volume 5. J. W. Shaw, editor. Plenum Publishing Corp., New York. 1–81.

74. Schnapp, B. J., R. D. Vale, M. P. Sheetz, and T. S. Reese. 1985. Single microtubules from squid axoplasm support bidirectional movement of organelles. *Cell.* 40:455–462.

75. Seybold, J., W. Bieger, and H. F. Kern. 1975. Studies on intracellular transport of secretory proteins in the rat exocrine pancreas. II. Inhibition by antimicrotubular agents. *Virchows Arch. Pathol. Anat. Histol.* 368:309–327.

76. Simons, K., and S. Fuller. 1986. Cell surface polarity in epithelia. *Ann. Rev. Cell Biol.* 1:243–288.

77. Simons, K., and G. Warren. 1984. Semliki Forest virus: a probe for membrane traffic in the animal cell. *Adv. Protein Chem.* 36:79–132.

78. Sitte, H. 1967. Morphometrische Untersuchungen and Zellen. *In* Quantitative Methods in Morphology. E. R. Wiebel and H. Elias, editors. Springer-Verlag, Berlin. 167–198.

79. Sobel, J. S., and M. A. Alliegro. 1985. Changes in the distribution of a spectrin-like protein during development of the preimplantation mouse embryo. *J. Cell Biol.* 100:333–336.

80. Strous, G. J. A. M., R. Willemsen, P. van Kerkhof, J. W. Slot, H. J. Geuze, and H. F. Lodish. 1983. Vesicular stomatitis virus glycoprotein, albumin, and transferrin are transported to the cell surface via the same Golgi vesicles. *J. Cell Biol.* 97:1815–1822.

81. van Os, C. H., M. D. de Jong, and J. G. F. Slegers. 1974. Dimensions of polar pathways through rabbit gallbladder epithelium. *J. Membr. Biol.* 15:363–382.

82. Wehland, J., M. Henkart, R. Klausner, and I. Sandoval. 1983. Role of microtubules in the distribution of the Golgi apparatus: effect of taxol and microinjected anti-a-tubulin antibodies. *Proc. Natl. Acad. Sci. USA.* 80:4286–4290.

83. Weibel, E. R. 1969. Stereological principles for morphometry in electron microscopic cytology. *Int. Rev. Cytol.* 26:235–302.